

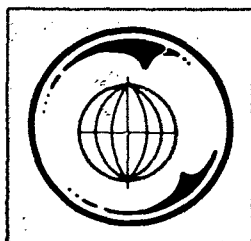
ANALYSIS OF SYNTHETIC APERTURE RADAR IMAGERY

Principal Investigator
Bruce J. Blanchard
Remote Sensing Center
College Station, Texas 77843

June 10, 1977
Final Report for Period
May 1976 - June 1977

Prepared for
Goddard Space Flight Center
Greenbelt, Maryland 20771

Contract No. NAS5-23458



TEXAS A&M UNIVERSITY
REMOTE SENSING CENTER
COLLEGE STATION, TEXAS



REPRODUCIBLE COPY
FACILITY CASEFILE COPY

ANALYSIS OF SYNTHETIC APERTURE RADAR IMAGERY

Principal Investigator
Bruce J. Blanchard
Remote Sensing Center
College Station, Texas 77843

June 10, 1977
Final Report for Period
May 1976 - June 1977

Prepared for
Goddard Space Flight Center
Greenbelt, Maryland 20771

Contract No. NAS5-23458

TABLE OF CONTENTS

<u>Section</u>	<u>Page</u>
TABLE OF CONTENTS.	i
LIST OF FIGURES.	ii
LIST OF TABLES	iii
<u>INTRODUCTION</u>	1
<u>OBJECTIVES AND APPROACH OF THE STUDY</u>	6
<u>ERIM Data Collection and Preprocessing</u>	8
<u>Jet Propulsion Laboratory</u> <u>Radar Data.</u>	11
<u>Watershed Surface Conditions.</u>	12
<u>GENERAL OBSERVATIONS OF THE RADAR IMAGERY.</u>	13
<u>DENSITY MEASUREMENTS OF THE IMAGES</u>	17
<u>DIGITAL DATA ANALYSIS.</u>	19
<u>CONCLUSIONS.</u>	34
REFERENCES	35

LIST OF FIGURES

<u>Figure</u>		<u>Page</u>
1.	Location of Radar Imaged Area	10
2.	ERIM X-Band Cross Track Plots of Along Track Average from Digital Radar Values.	21
3.	ERIM L-Band Cross Track Plots of Along Track Average from Digital Radar Values.	22
4.	Comparison of L-Band, Like Polarized, Cross Track Averages for Two Systems. . . .	23
5.	Grey Scale Maps of ERIM, Raw Digital Data Over Small Rangeland Watersheds. . . .	27
6.	Grey Scale Maps of ERIM, Digital Data Over Small Rangeland Watersheds Corrected for Cross Track Pattern Differences.	29
7.	Comparison of Grey Scale Maps of ERIM and JPL, L-Band Like Polarized Digital Data Over Small Rangeland Watersheds After Corrections	30
8.	Graphical Illustration of the Relation Between Average Digital Radar Data and Watershed Runoff Curve Numbers.	33

LIST OF TABLESTablePage

- | | | |
|----|---|----|
| 1. | Average Digital Values and Runoff
Curve Numbers for Rangeland Water-
sheds. | 26 |
|----|---|----|

ANALYSIS OF SYNTHETIC APERTURE RADAR IMAGERY

INTRODUCTION

Differences in surfaces of watershed drainage basins have a dominant effect on the proportion of rainfall that can be stored or detained in the near surface zone of the soil-air interface. Rainfall that cannot be stored or detained flows through the drainage pattern and converges in the main stream channels to produce flows that when excessive, are commonly thought of as floods. The control and management of stream flow is of utmost importance to the optimum use of water supplies and the prevention of flooding catastrophies.

One of the more common techniques for evaluating the surface conditions of a watershed was developed by the Soil Conservation Service (SCS). This technique centers around a simple emperical equation for predicting storm runoff in which rainfall and a watershed runoff coefficient called a "curve number" are used as inputs. Rainfall inputs are estimated for the drainage area from point rainfall data available from the nearest National Weather Service rain gauges. The curve number is developed from a complex set of tables that relate the hydrologic classification of the soil, the vegetation type, the tillage practice and the antecedent moisture conditions to the curve number.

Past study and extensive experience with the use of this technique has indicated that the permeability of the soil and the density and stage of growth of vegetation are the major components of the storage represented by the curve number. In most instances the major portion of watersheds of interest are not intensively tilled, therefore, tillage practices do have some influence on local surface detention if the area in question is farmed with good conservation practices, contour tillage, terracing, etc. Antecedent conditions are also of some importance, however, the effects of the antecedent moisture conditions are closely tied to the drainage or permeability of the soil.

By virtue of the fact that fast drying soils reflect more visible light than slow drying soils and the fact that differences in vegetation type and volume also influence reflectance of visible light it would seem that the curve number could be classified by visible light imaging. This approach was tested in a study using Landsat data over well instrumented watersheds (1). The classification proved valid under some extremely restrictive conditions. First the watersheds must be imaged under dry conditions and secondly, the vegetation must be dormant. The technique was tested on several watersheds where major portions of the drainage areas had moderate stands of dormant scrub oak timber. When either moderate moisture or growing vegetation existed the technique did not

work. This would imply that soils conditions or the storage capacity of the soil was essentially masked by growing vegetation.

To overcome the masking effect an attempt was made to classify runoff curve numbers with the Passive Microwave Imaging System (PMIS) (2). This system was used in an experiment conducted in 1972, primarily because it was the only available microwave sensor that scans at a constant angle. It was recognized at that time that microwave sensors in general had the ability to sense conditions in the near surface soil zones. This particular sensor is X-band (2.8cm wavelength) which implied that it could probably only penetrate one to two centimeters in depth and could not at the designed look angle, 49 degrees off nadir, penetrate vegetation.

The experiment with the PMIS was performed over watersheds in the same study area used for the Landsat study mentioned earlier. Two separate sets of data were collected. One set was collected in the dormant spring and the second set in summer. Both sets of data were collected when moderate soil moisture conditions prevailed over the drainage areas. The moderate moisture conditions did not influence the good relation found between horizontal polarized antenna temperature and SCS curve numbers. The growing vegetation in the summer did, however, mask the surface and resulted in a drastically reduced sensitivity of the antenna temperature to differences

in SCS curve numbers.

These experiments led to the conclusion that microwave systems held promise for eliminating at least the dry soil restriction evidenced in the visible light study. The results also implied that to provide a system that would be more universally usable, a portion of the microwave spectrum should be used that would penetrate at least moderate volumes of vegetation and be responsive to differences in soil condition.

Microwave systems in general are sensitive to soil moisture to some depth below the surface of bare ground. Theoretical and some field studies have demonstrated that the effective depth of penetration is a function of wavelength and the moisture content of surface soils. At the same time sensitivity to soil conditions under vegetation has been demonstrated by experiments with truck mounted systems when longer wavelengths and steep look angles are used. (3,4) These capabilities indicate that it might be possible to sense the water storage potential in soils that are not near saturation. Soils that are well drained or permeable should look dry before nearby soils that are impermeable. The relative dryness of the soil should in turn be related to the differences in storage available for rainfall on the surface.

Microwave systems are also sensitive to roughness that in the bare ground areas is the actual physical irregular-

ities in the surface. The roughness seen in vegetated areas is more related to the scattering of microwave energy by the vegetation. Roughness sensitivity is also dependent on wavelength and look angle. Physical measurement of roughness has been difficult, therefore, limited information is available for quantifying roughness of natural terrain and vegetation at different frequencies and look angles.

As SCS curve numbers are primarily dependent on soils characteristics, vegetation density and types vegetation, it seems reasonable that a remote sensing system capable of estimating such values must include a sensor capable of sensing soil under average vegetation and at the same time capable of estimating vegetation volume.

A dual frequency radar with appropriate frequencies and look angles should offer the capability for such measurements. One frequency should have the ability to penetrate the vegetation while the other should be capable of recognizing differences in the vegetation density.

The only dual frequency radar imager available at the time of this experiment was a Synthetic Aperture Radar (SAR) with X and L-band frequencies that receives like and cross polarized data simultaneously in both frequencies. This system produces data onboard and stores the data on signal film. The antenna array is mounted on the underside of a C46 Curtis aircraft on a gimbeled mounting and can be aligned

with the flight path to compensate for drift. The entire array is covered with a radome to protect the antenna. Prior to the initiation of this study an attempt had been made to calibrate the cross track antenna pattern for this particular system. Calibration measurements were made by flying repeated lines over a known target. This type of calibration is expensive and the measurements are difficult to obtain therefore the number of calibration points in the antenna pattern were limited.

OBJECTIVES AND APPROACH OF THE STUDY

As a result of the logic followed in the prior discussion, a study was initiated to examine the capability of a dual frequency SAR over a watershed study area.

The study was directed toward demonstrating the capability of radar systems to recognize contrasts between watersheds with different runoff potential. SAR data were collected by the Environmental Research Institute of Michigan (ERIM) using their aircraft system over watersheds being monitored by the USDA - Agricultural Research Service (ARS). In addition, the Jet Propulsion Laboratory (JPL) of Pasadena, California furnished L-band radar data with this same study. These data were to be analyzed to determine if the radar response of the longer wavelength in the microwave region, L-band and/or X-band, can be related to the runoff curve number used in the SCS watershed runoff equation. It was also

an opportunity to determine whether the L-band system could provide the desired penetration of vegetation.

It was proposed that the SAR data would be provided by ERIM on film strips and the density measurements of the film would be examined to determine if conventional hydrologic parameters could be detected in the data. Watershed drainage areas for the selected watersheds having extensive historical records of rainfall and runoff were to be mapped to identify the radar data within the watershed boundary.

The average density of strips of data representing a narrow range of angle off nadir were to be modified to correct for differences in radar power. An average modified return was to be compared to watershed runoff coefficients derived from the rainfall and runoff data. The work required to complete this study was envisioned as three related tasks.

1. Locate the specific watersheds on the four channels of SAR imagery. The four channels are the like and cross polarized returns at X and L-bands.

2. Determine the average values in a relative sense of the backscatter coefficients for these watersheds. If possible, the effect of the varying nadir angle on the scattering coefficient would also be determined.

3. Correlate the observed scattering coefficient with known watershed parameters for those watersheds and with ground observations made at the time of the flight.

Precipitation data from a dense network of recording gauges was also to be acquired from the Agricultural Research Service in order to estimate soil moisture influence on the radar backscatter. These data were to be used to supplement data collected for other soil moisture studies at Columbia, Missouri, St. Charles, Missouri and at Lafayette, Indiana.

ERIM Data Collection and Preprocessing

The ERIM System was flown over a series of parallel flight lines (Figure 1) arranged to provide coverage of some watersheds as large as 70 sq. mi. (181 km^2) while also imaging four small watersheds at two or three look angles. These data were collected on November 11, 1975 with no apparent problems in the operation of the system.

The SAR data were recorded on signal film that was then optically correlated by ERIM personnel. The ERIM optical correlation can be used to produce either image film or digital data at the output plane. Image film was produced for all of the data after the principal investigator had examined test runs on both like and cross polarized data. The light source on the optical bench was increased to maximum intensity for processing cross polarized data. Otherwise, data for the entire mission were processed alike for each flight line.

The increase in the light source intensity essentially shifts the data up approximately 4.8 db thus making the contrast between different surfaces more visible on the image. The need for the shift is due primarily to the overall reduction of power in the cross polarized return.

The reader should recognize that the operation of an optical correlator produces subjective data in a certain sense. The operator must make numerous adjustments on elements of the light bench to try to optimize the retrieval of the maximum value present in the signal film. Some minor adjustments can influence the end product, and since the adjustments are made manually, repeatability in quality depends on the skill of the operator. Since the input and output for the image film product are subject to quality of film and developing, more opportunities for differences in data are present in image film systems. Extreme care was taken by ERIM personnel to minimize the possible errors in this data set.

The digitizing technique used by ERIM records the image directly on the output end of the optical bench. This technique is appealing as opposed to digitizing the imagery, since the opportunity for error is reduced. As this study progressed, some selected areas over the study watersheds were digitized to aid in data manipulation to try to compensate for the irregular antenna pattern. Estimates of the

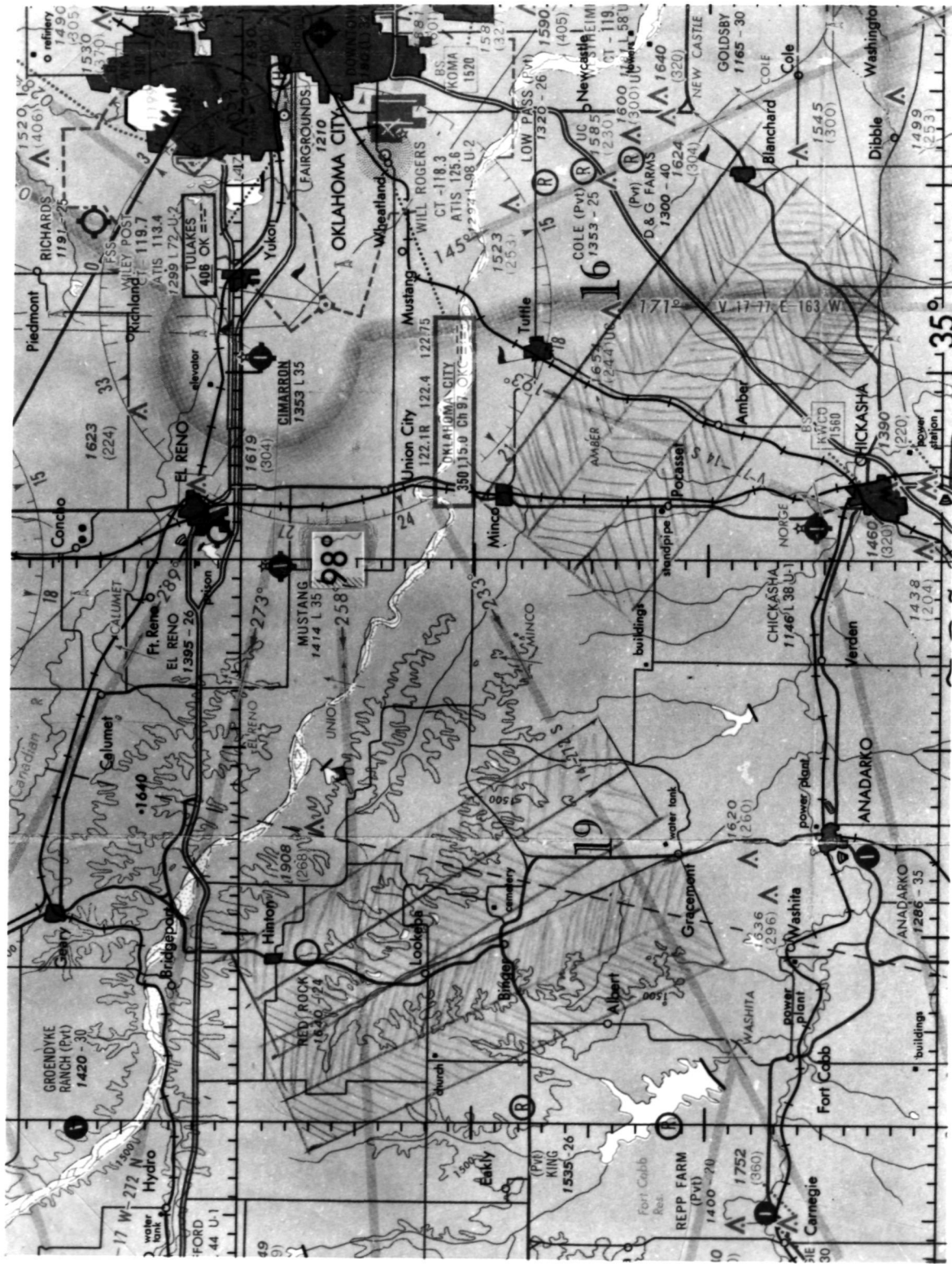


Figure 1. Location of Radar Imaged Area

antenna pattern and the limited set of calibration data were supplied by ERIM to aid in interpretation of the data. Numerous helpful conversations with ERIM personnel concerning the data processing techniques also provided aid in developing programs to correct the data for some antenna pattern irregularities.

Jet Propulsion Laboratory Radar Data

On January 6, 1976 the JPL/SAR system on the NASA-990 aircraft was flown over some of the same watershed areas. Only L-band data was available from this flight and some problems were experienced with the L-band cross polarized data. Quality of the like polarized data is excellent from this flight. Sub areas of these data were digitized at JPL and displayed on the analyses system in their laboratory for the benefit of the investigation.

At the time these data were processed the digitizing system used by JPL did not record data directly from the optical correlator. There was, therefore, the added steps where film images were produced, then density of the film was digitized.

Other distinct differences between the ERIM and JPL data are the fact that the antenna of the JPL system is not covered with a radome and directional stability of the antenna is controlled by flying at high altitude where little turbulence is experienced. Data from this system may

more nearly approximate spacecraft radar results where the antenna will not be covered with a radome.

Watershed Surface Conditions

Surfaces of the watershed areas imaged are primarily devoted to grazing land and some upland wheat. Parts of the western portions of the study area have light to moderate stands of scrub oak timber and some of the uplands in this area were bare fields where peanuts had been harvested in the fall. The eastern portions are predominantly Chickasha and Marlow formations of the Permian Red Beds while the western flight lines cover areas that are primarily Rush Springs sandstone. The soils developed from these formations are sandy and permeable on the west and silty clay impermeable soils in the east portion of the area. The entire imaged area in Oklahoma was dry and only insignificant differences were found in antecedent rainfall for the preceeding thirty days.

Four small rangeland watersheds in the east end of the study have been used as prime sites in previous remote sensing studies. These watersheds are characteristic of the extremes in rangeland runoff. Two of the watersheds (R5 and R6) are located on prairie soils that have been maintained in native grasses. Hence, the original topsoil has been preserved. The two remaining watersheds (R7 and R8) are located on an adjacent farm and were plowed and cropped for several years. Topsoils on these two watersheds have

been eroded away and the land was allowed to revert to poor native pasture. The two watersheds on good soils have produced approximately one tenth as much runoff as the watersheds on eroded soil.

No green growing vegetation was evident within any of these watersheds when radar flights were made. There was, however, considerable differences in the volume of dormant grass. Watersheds R5 and parts of R7 had been fertilized in the prior growing season. An exceptionally dense growth of native grass was present on R5. Moderate improvement in vegetation density occurred on R7 in response to the fertilizer, but the cover was not as good hydrologically as the cover on the R6 untreated watershed.

Hydrologic measurements began on these small watersheds in 1966 and are still continuing. Records from 1966 through 1974 were used in this study.

GENERAL OBSERVATIONS OF THE RADAR IMAGERY

Imagery from the ERIM system was provided as film negatives for each flight line in strips 4.5 cm wide. The most dominant difference between the X and L-band data is the response in the two bands to roughness of the surfaces and vegetation.

Differences in the density across track are indicative of the relative power in the antenna pattern. As would be expected, the regions near the center of the antenna beam show good contrast between different surfaces, particularly in the cross polarized image. The reduction in power returning in the cross polarized data expands the range of signal across track to such an extent that the distinction of contrasting fields is seriously impaired in the near nadir and far angles. Film density readings for different look angles are difficult to compare on such imagery as there is no valid way to rebuild the range of return that existed in the original radar signal film.

Other contrasts in density across track are evident in the cross track direction of the ERIM L-band like polarized data. These differences become evident when viewing the image from one end of the flight direction and are attributed to irregularities in the antenna pattern. When viewed across track, these irregularities at first seem related to differences in surface slopes. Close examination does reveal some effect of surface slope, particularly in the like polarized data for both X and L-band data. The slope effects are not readily apparent in the cross polarized data.

Slope effects help to enhance the data for many uses, however, differences in film density due to irregularities in the antenna pattern are detrimental. An attempt to

rectify some of the later irregularities when compiling film density measurements from specific target areas that were imaged at different look angles proved discouraging. Observations made while measuring film density in this imagery indicate that when the image is once transferred to the film state, the data from weak areas in the antenna pattern is reduced in value. In contrast to this situation, digital data of the same image plane allows a wider range of numbers and even though the along track power may be reduced, the data may exhibit a greater portion of its original dynamic range.

Other irregularities in density were evident in the X-band ERIM data along the flight path. These can be attributed to rough flying conditions beyond the capacity of the gimballed antenna mount. The along track density differences are not significant with regard to the analyses of these data as they occurred in areas of little importance. This problem will not likely occur when the system is flown at high altitudes or in non-turbulent weather.

The L-band ERIM, like polarized imagery, shows less contrast between fields of different crops and surface roughness than is evident in the L-band cross polarized images. One must keep in mind that when the data were correlated that the light source in the optical processing was increased for the cross polarized data. Had this not been

done, much of the contrast and overall information content in the cross polarized data would have been lost.

No difference could be detected in L-band images between average grazed native grass pastures and adjacent winter wheat fields. Sharp contrasts between these types of vegetation are evident in the X-band data. This bears out the possibility that the longer wavelength of the L-band system is capable of penetrating moderate vegetation. In the ERIM L-band data, increased scattering does occur when excessively heavy native grass areas are imaged. In one of the small rangeland watersheds heavy application of fertilizer was made on good range. Grazing was restricted for a period of several months prior to the radar flights and native grass was extremely dense and more than one meter in height. This difference in vegetation volume can be identified in each of the ERIM images but cannot be seen in the JPL, L-band image.

Good definition on land-water boundaries is evident in the X-band like and cross polarized data. The identification of small farm ponds is particularly easy with these images while in the L-band images ponds can easily be misinterpreted as pastureland. In another image of an area in the St. Charles, Missouri region, ponded water under a forest cover of dormant hardwoods produced a marked change in the backscatter in relation to adjacent areas of timber. These observations are contradictory in a sense and should

be investigated in other data since the definition of flooded areas is an important radar application.

It is also evident in these data that backscatter from eroded areas in fields and bare gullies can easily be misinterpreted as timber or brushy areas. This confusion factor may influence the interpretation of images over geologic domains that are easily eroded when comparing the data to images of little or no erosion.

Response from timber and brush is similar in both bands. In the L-band data the trees along the drainage pattern helps to define the watershed areas. Some portions of the L-band data from outside the Chickasha watershed study area were completely covered with timber. Differences in types of trees in these areas can be detected in the data.

DENSITY MEASUREMENTS OF THE IMAGES

An effort was made to find correlations between film density and some hydrologic characteristics such as soil moisture, soil permeability and density of crop or range-land cover. Maps were prepared of the imaged area to locate rain gauges, fields of wheat, bare soil and native grass that could be qualitatively assessed from observations on the ground or from recorded measurement. Little difference in antecedent rainfall existed over the area imaged, thus, there was no real opportunity to evaluate soil moisture measurement capability.

Also the useful portion of the radar swath was imaged at larger angles than those desirable for soil moisture measurement.

The density measurements when comparing bare ground fields indicated that most contrasts between field was related to the tillage and the associated roughness. Fields of relative dry winter wheat could not be distinguished from bare ground that had been tilled with a spring tooth harrow. Fields that had recently been plowed were relatively rough and could easily be identified by differences in film density in relation to other fields.

Density measurements were plotted for bare soil, wheat and pasture versus the distance across the film to get some estimate of the influence of antenna pattern differences. These plots were compared with estimates of the actual antenna pattern supplied by ERIM. Differences in density due to power distribution in the pattern were on the order of four to ten times as large as differences in density from fields with like crop along a single look angle. Corrections in density were made for an arbitrary antenna pattern and the points were re-plotted. The range of adjusted density for all three surface conditions overlay each other at all look angles. This result was interpreted as an indication that after antenna power corrections were made the remaining differences in density were caused primarily by differences in roughness and since

the ranges of density for bare ground, wheat and rangeland overlap there is little reason to expect reliable separation of these three surfaces.

A check of film quality by comparison of densitometer measurement of the density wedges was made and the various strips compared well. This indicated the film quality and film processing was uniform. Since the quality of the data in the signal film looked much better than the image film the decision was made to digitize portions of these data in an attempt to improve the data product.

DIGITAL DATA ANALYSIS

The principal area selected for processing into digital data for both the ERIM and JPL data covered the location of four intensely monitored small watersheds described previously. The ERIM data were digitized on the image plane of the optical bench whereas the JPL data were digitized from film.

The digital data were examined for differences across track created by fluctuations in the antenna power. Average values along track were calculated for each file. Examples of the averages are shown in Figures 2, 3 and 4. Modification of the digital data was then made by normalizing the digital values to the mean value calculated for a point twenty degrees off nadir. This modification can only enhance the image by correcting for the cross track variations in the

antenna pattern. Similar irregularities should be expected in the along track pattern, however, distortion of the data in that direction cannot be removed after the optical correlating operation.

Pattern illustrations such as those in Figures 2 through 4 do not remain constant over terrain that is not uniform. To make corrections of this type, averages obtained over uniform targets such as water with uniform roughness would be more useful. Data over water was not available for this study. These figures do illustrate the great difference in one way patterns of the X and L-band ERIM system. Considerable difference between the ERIM and JPL L-band like polarized antenna patterns is also evident in Figure 4.

It may not be reasonable to assume the patterns illustrated in Figure 4 are different solely as a result of the antenna design because the ERIM system is flown under a radome while the JPL system is not. Some of the difference in apparent pattern may be due to radome interference.

The patterns and the inherent problems of correction serve to point out that precise quantitative measurements from radar are more likely to be obtained by restricting the collection of data to a narrow range of angles and by direct digital processing of data. This can only be accomplished for large areas by using spacecraft platforms. The problems associated with making corrections along track lead to the

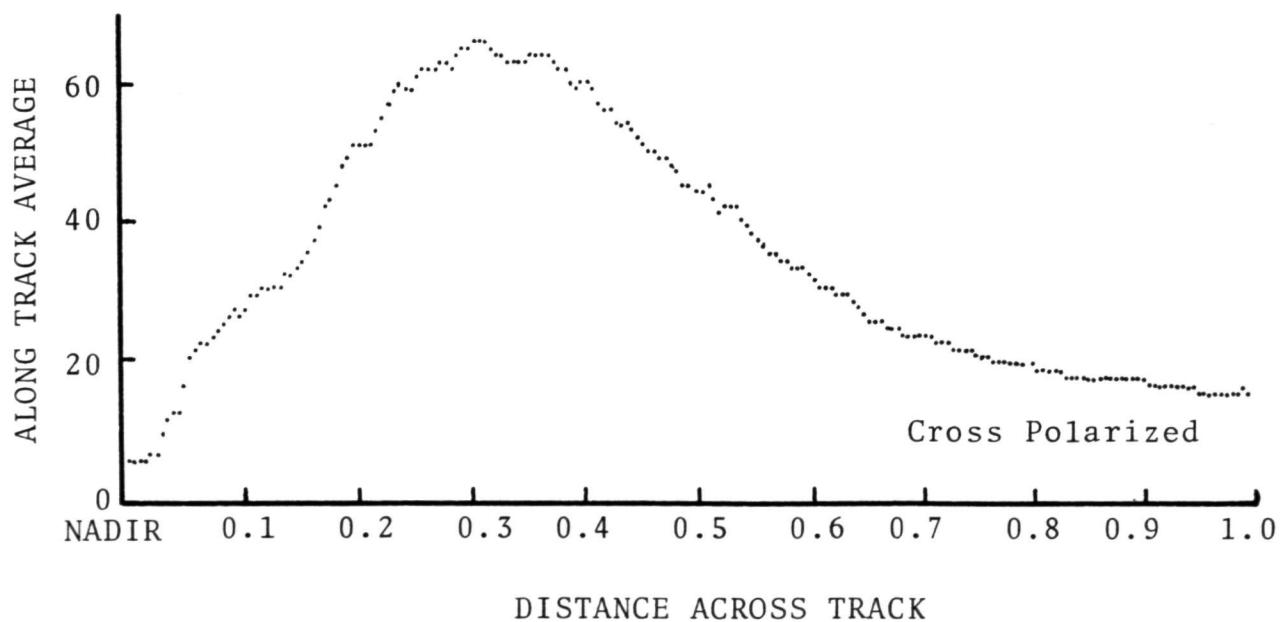
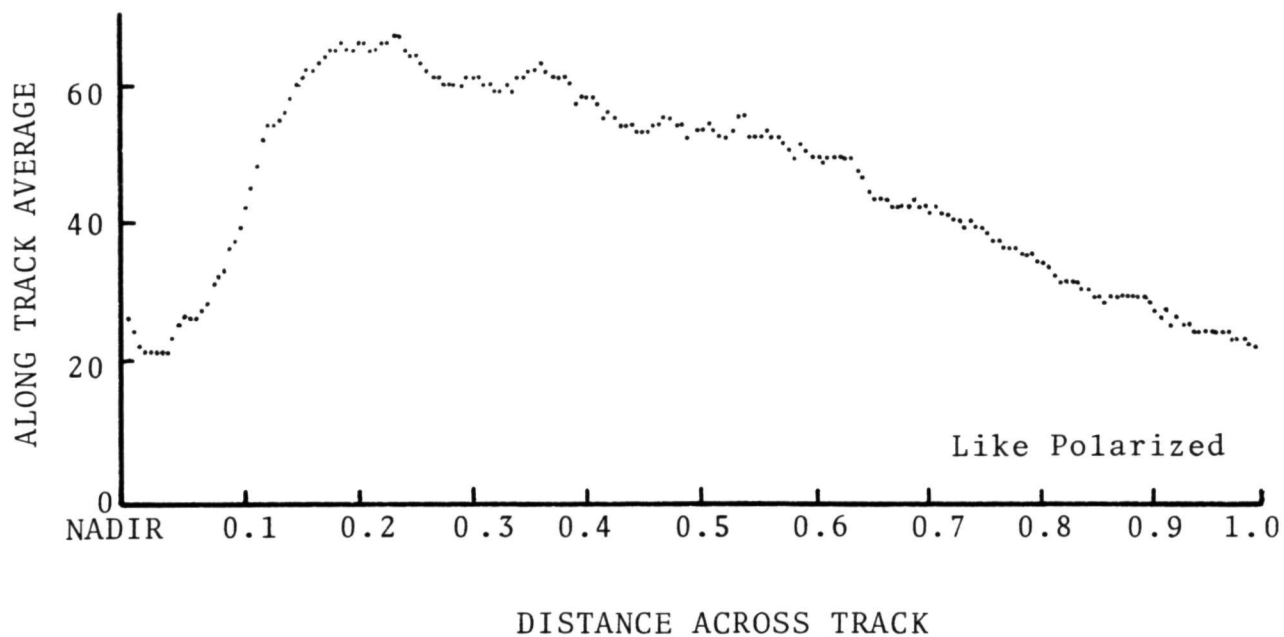


Figure 2. ERIM X-Band Cross Track Plots of Along Track Average from Digital Radar Values

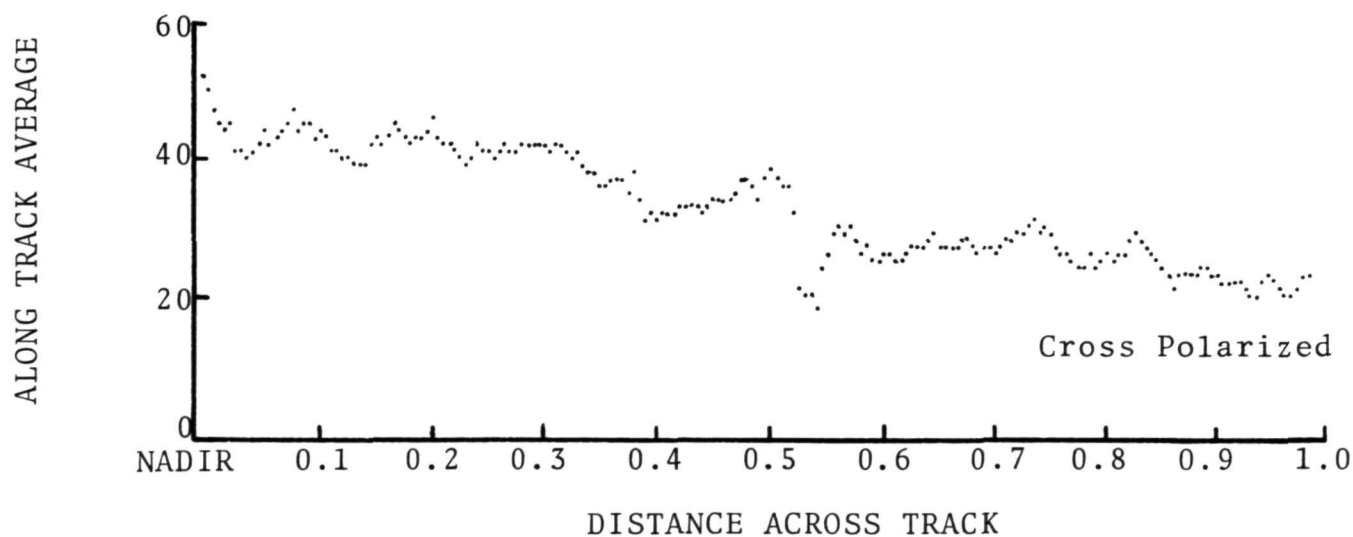
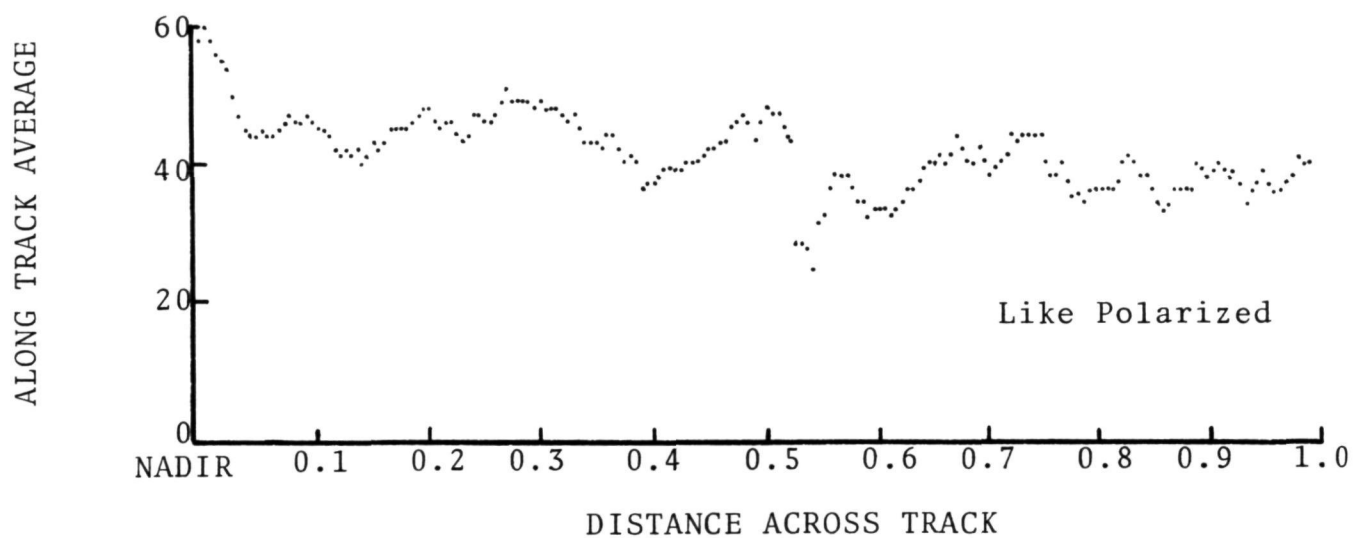


Figure 3. ERIM L-Band Cross Track Plots of Along Track Average from Digital Radar Values

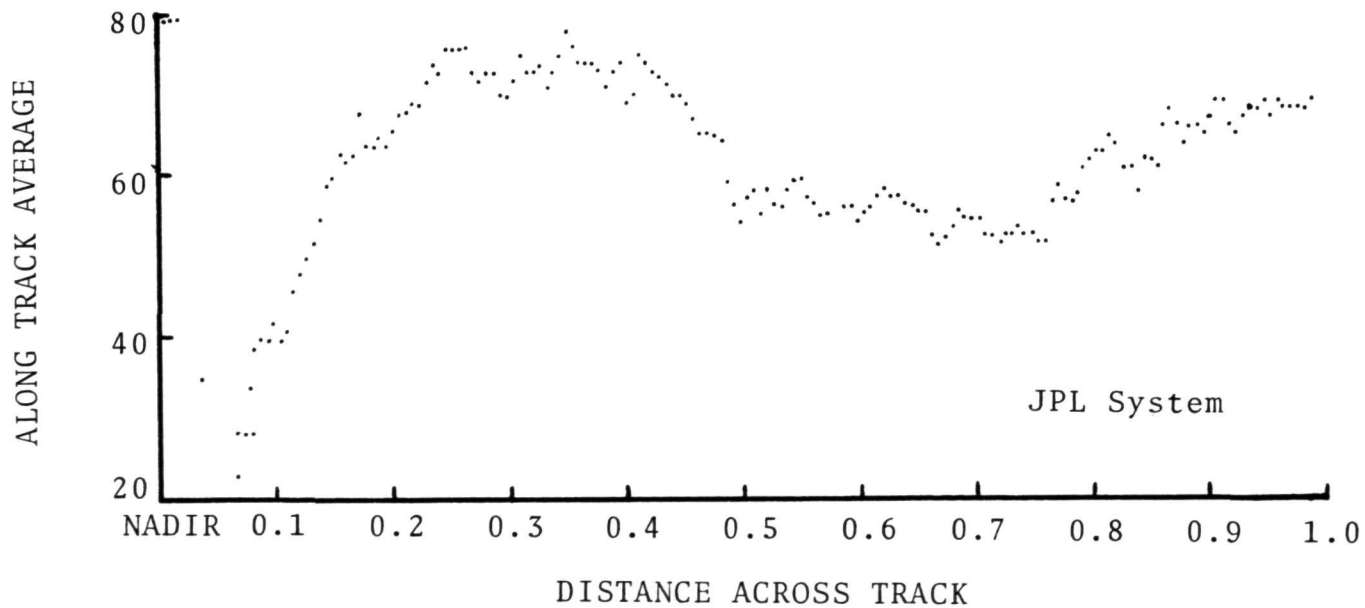
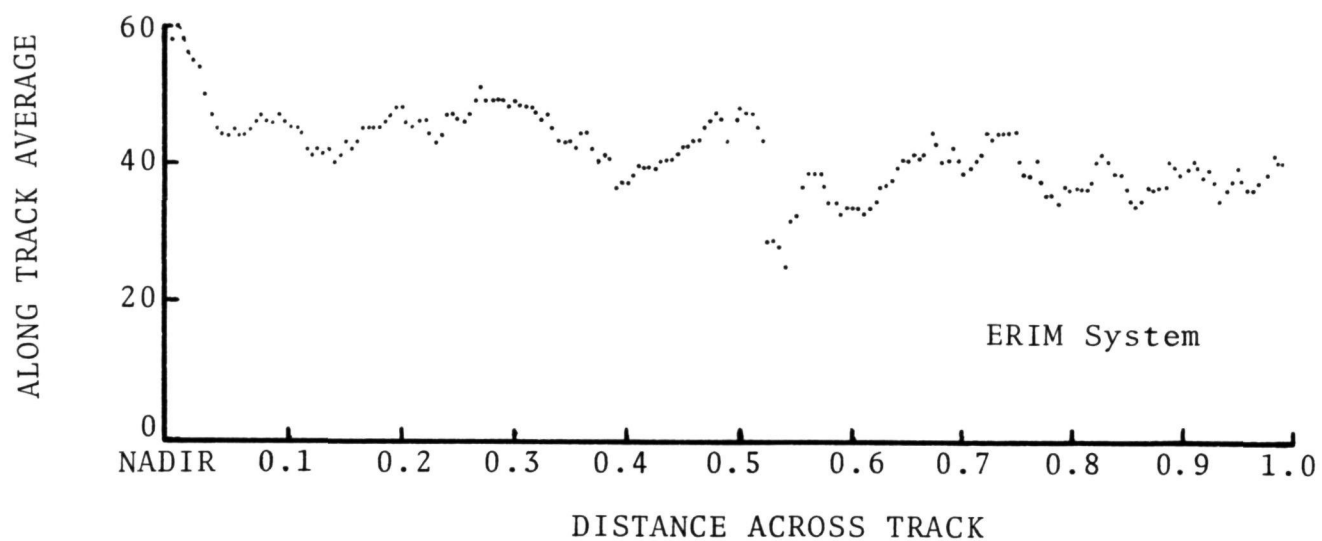


Figure 4. Comparison of L-Band, Like Polarized, Cross Track Averages for Two Systems

conclusion that precise measurement of the antenna pattern should be made before development of the data processing system even for spacecraft radar.

Consideration of the above problems in the data led to a decision that averages over large watersheds representing a wide range of look angles might be suspect. Further data processing was then confined to the four small rangeland watersheds located in the area of less than one square kilometer. Unfortunately, these watersheds were imaged at angles farther off nadir than desirable. In the ERIM data the watersheds were imaged at approximately 48 degrees off nadir and in the JPL data the same watersheds were imaged at approximately 42 degrees. All past experiments would indicate that differences in moisture at these angles should have no significant influence on the data.

The region around the watersheds was grey scaled to produce an image of the digital data in order to accurately define the watershed location. Boundaries of the watersheds were mapped on aerial color infrared film and then transferred to the grey scale images. Areas of timber in two of the watersheds were also defined on the grey scale images.

Digital data for the portions of each watershed drainage area that was not covered by timber were selected from the computer tapes and averaged for each watershed. A corner reflector had been placed at the top of the drainage

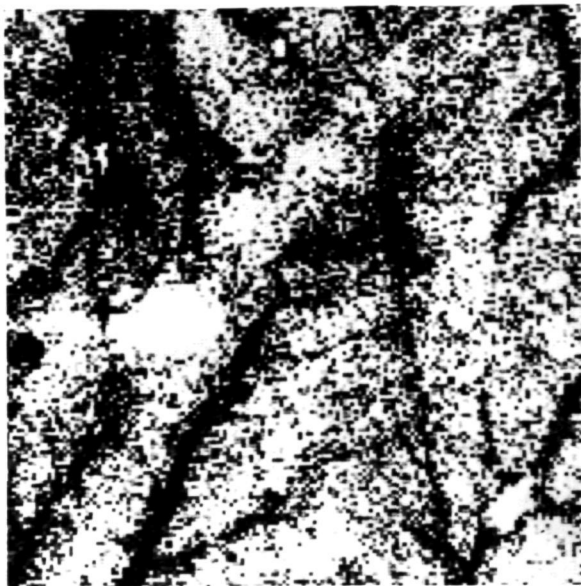
areas of R7 so a small portion of data influenced by the reflector was also deleted from the values used to compute averages. Table 1 is a summary of the average values calculated and the curve number for each watershed calculated from measured precipitation and runoff.

Grey scale illustrations of digitized data before any correction had been calculated for across track differences in antenna power are shown in Figure 5. In these images the darker tones represent surfaces where the microwave energy is scattered. The characteristic cross created by a corner reflector is evident near the center of the left edge in the X-band like polarized image. The reflector is not readily identifiable in the cross polarized image or in like or cross polarized L-band images. The white area in a tributary located in the lower right side of the image is a farm pond.

By using the boundaries shown in Figure 6, the test watershed areas can be located in Figure 5. Watershed R5 is noticeably darker in all the ERIM images indicating that the dense dormant grass was influencing the return. The location of a gravel section line road and a fence line between two farms are shown on one image in Figure 6. The cross polarized data that has been corrected indicates considerable difference in return on each side of the fence. The good hydrologic soils with low runoff characteristics are on the upper right side of the fence while eroded soils dominate the farm at the

<u>ERIM</u>	<u>WATERSHED NUMBER</u>			
	R 5	R 6	R 7	R 8
X Band Like Polarized	72.7	60.5	52.9	54.2
X Band Cross Polarized	54.5	42.5	36.6	33.6
L Band Like Polarized	52.6	46.7	37.2	46.1
L Band Cross Polarized	41.4	35.5	33.0	37.0
JPL				
L Band Like Polarized	126.5	131.4	90.6	78.7
SCS				
Curve Number	52.5	50.5	69.3	73.7

Table 1. Average Radar Digital Valves and Runoff Curve Numbers for Rangeland Watersheds



X-Band Like Polarized



X-Band Cross Polarized



L-Band Like Polarized



L-Band Cross Polarized

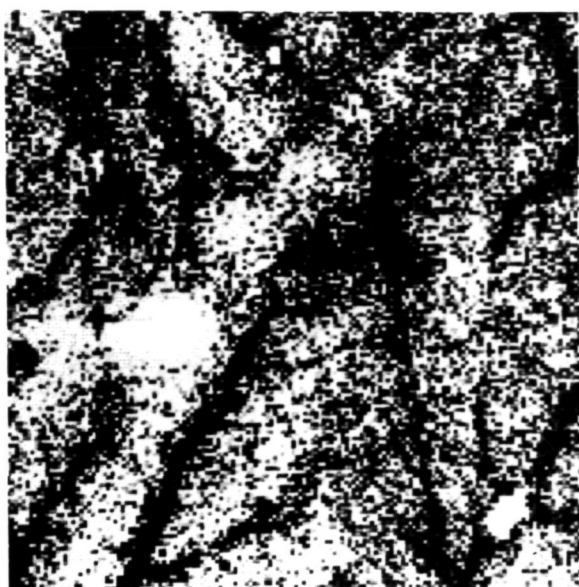
Figure 5. Grey scale maps of ERIM, raw digital data over small rangeland watersheds.

lower left side of the fence. High scatter is evident over the low runoff condition.

Differences between watersheds R5 and R6 within the low runoff area can be detected by increased scattering where dense vegetation occurred on R5. It appears that the difference across the fence line is primarily due to differences in volume of vegetation. Evidence from previous truck mounted microwave system measurements would lead one to expect active microwave response at look angles near 45 degrees of nadir to be primarily sensitive to roughness. These images substantiate the prior experience and show the cross polarized return for both X and L-band appears to be more sensitive to differences in rangeland vegetation volume than like polarized data.

Figures 5 and 6 also illustrate that timbered creek channels appear wider in the L-band data. Examination of the data reveals that this effect may result from processing differences. In these data there are more L-band data points that fell beyond the saturation level where real differences in the radar return cannot be distinguished. Direct digitization of the radar signal would eliminate this problem.

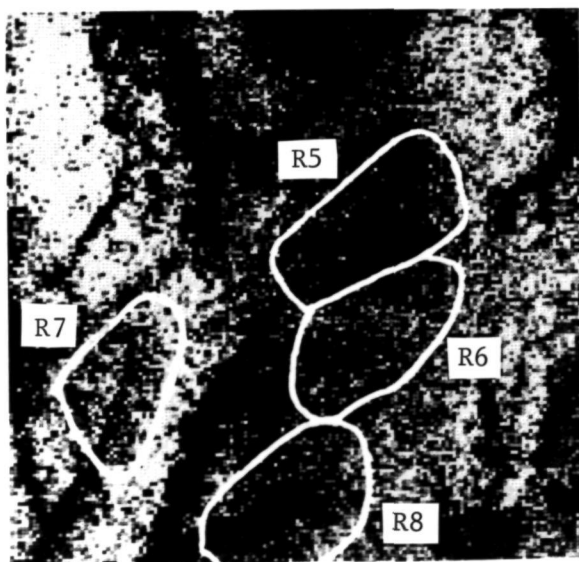
In Figure 7, contrasts between watersheds within both L-band data sets show that the JPL, L-band data for watersheds R5 and R6 are very near alike. Some grazing of the dormant grass on these areas was allowed during the seven week period between data sets. The volume reduction in



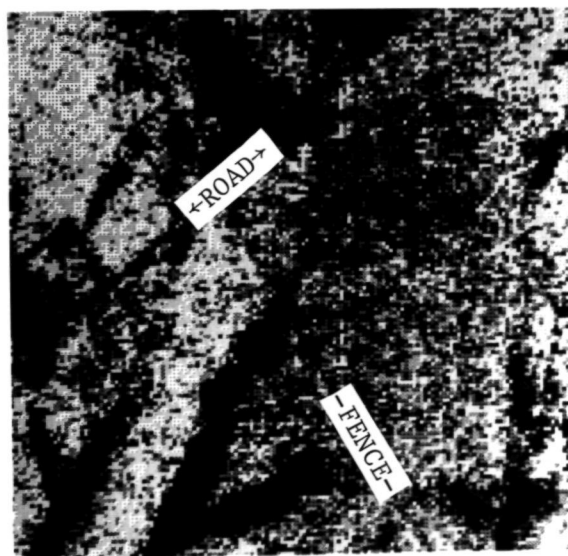
X-Band Like Polarized



X-Band Cross Polarized

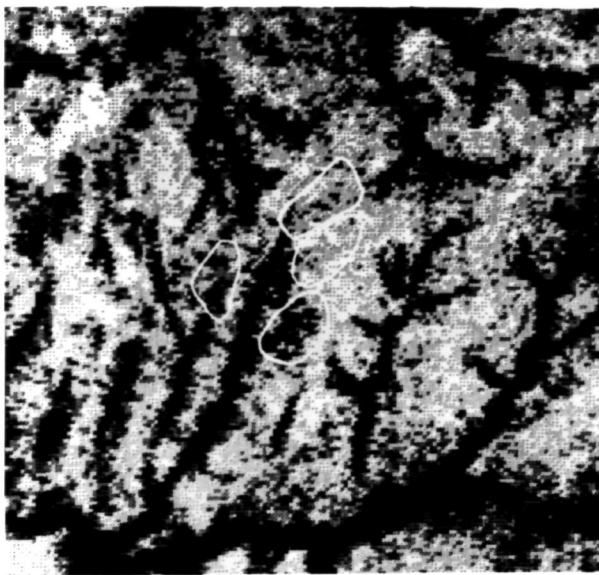


L-Band Like Polarized

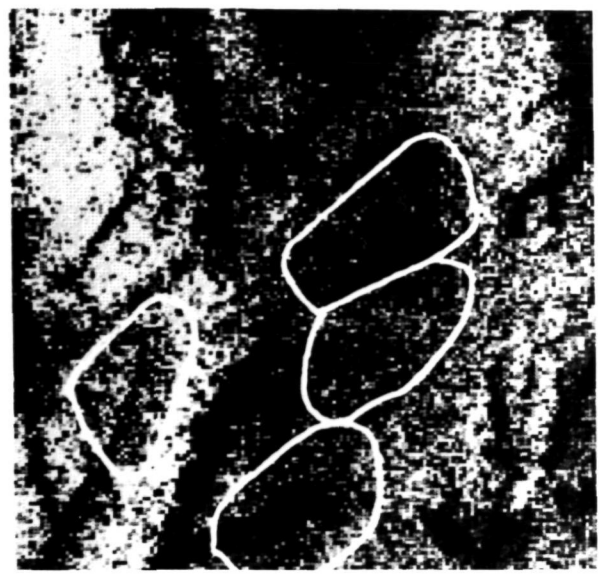


L-Band Cross Polarized

Figure 6. Grey scale maps of ERIM, digital data over small rangeland watersheds corrected for cross track pattern differences.



JPL



ERIM

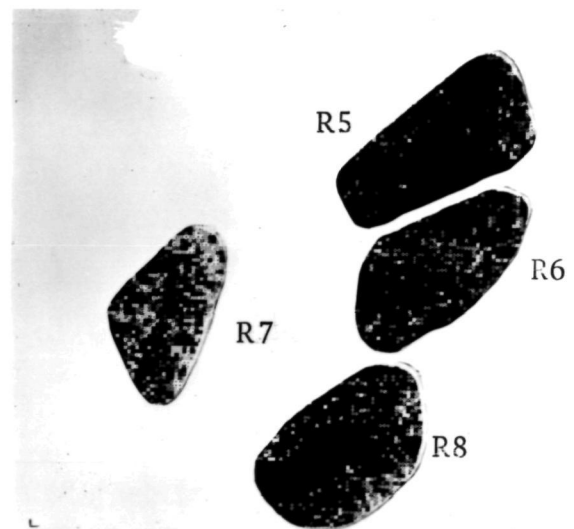
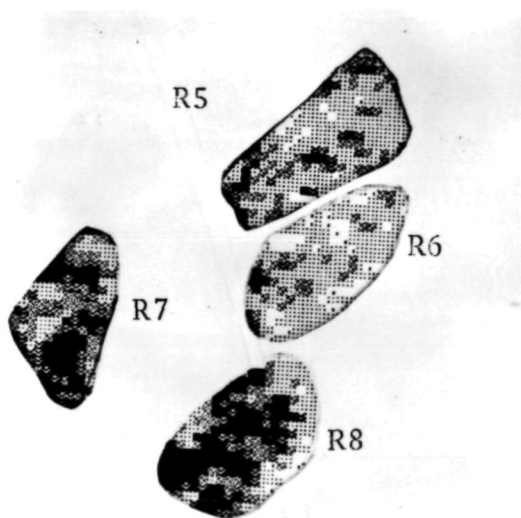


Figure 7. Comparison of grey scale maps of ERIM and JPL, L-Band like polarized digital data over small rangeland watersheds after corrections.

grass was most likely greater on R5 due to increased palatability from fertilizer. Vegetation on R5 was clipped, dried and weighed from 25 points on November 12, 6300#/acre of dry weight was measured while five days later similar sampling on R6 indicated 3500#/acre of dry weight. A series of sampling showed consumption on R5 was 500#/month, thus, there was at least one ton more vegetation per acre on R5 at the time of the JPL flight. The volume of standing vegetation on R5 was still extremely dense in the early spring when the grass was shredded to allow new growth. Accordingly the radar return should be expected to show a difference between R5 and R6. A repetition of the JPL flight has not been made, therefore it has been impossible to check the possibility that this sensor was able to penetrate even the dense native grass.

Values from Table 4 were used to develop the graphical illustration in Figure 8. The average curve numbers for each watershed were based on storms that occurred over an eight year period prior to the growth of the extremely heavy vegetation on watershed R5. No significant storms occurred on this watershed while the dense vegetation existed, thus, there are no measurements to indicate how much the curve number was reduced by the increase in vegetation.

If only the other three watersheds are considered, the only consistent decrease in digital counts with increasing curve number occurred in the X-band cross polarized data when

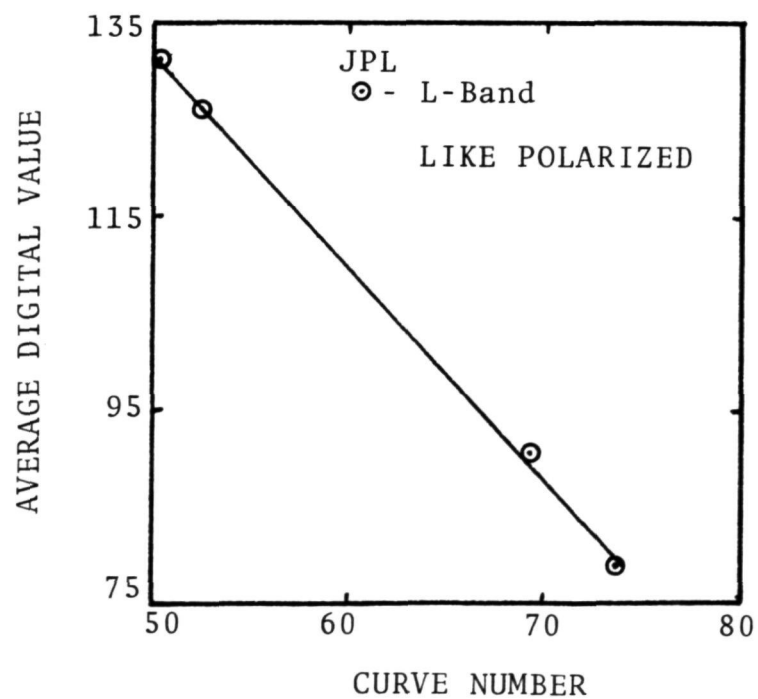
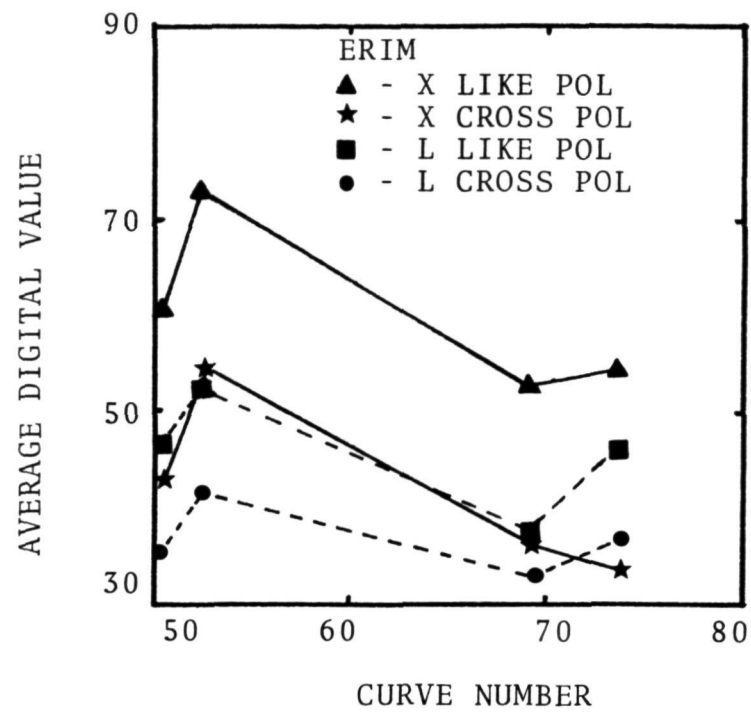


Figure 8. Graphical illustration of the relation between average digital radar data and watershed runoff curve numbers.

ERIM system was used. Considering both the X- and L-band data, the top figure indicates that bands are responding to the vegetation differences rather than differences in soils. In contrast to this the plot of the JPL data does not show the sensitivity to vegetation density and might therefore be measuring differences in soils.

CONCLUSIONS

This study has helped bring to light some of the following problems that will be faced in applications of radar measurements in hydrology.

1. Adequate calibration of the radar systems and direct digital data will be required in order that repeatable data can be acquired for hydrologic applications.

2. Quantitative hydrologic research on a large scale will be prohibitive with aircraft mounted synthetic aperture radar systems due to the system geometry, antenna pattern problems and overall cost of operation.

3. Spacecraft platforms appear to be the best platforms for radar systems when conducting research over watersheds larger than a few square kilometers.

4. Experimental radar systems should be designed to avoid use of radomes if at all possible.

5. The differences that occur in SCS curve numbers due to differences in vegetation volume appear to be detectable with X-band systems and the ERIM, L-band system.

6. Cross polarized X- and L-band data seem to discriminate between good and poor hydrologic cover better than like polarized data.

7. The JPL, L-band system appears to be primarily sensitive to differences in soils and possibly should be tested over small watersheds again.

REFERENCES

1. Blanchard, B.J., 1975. "Investigation of Use of Space Data in Watershed Hydrology." Final Report, Contract S-70251-AG., USDA-ARS, Chickasha, Oklahoma, p. 113.
2. Blanchard, B.J., J.W. Rouse, Jr., and T.J. Schmugge 1975. "Classifying Storm Runoff Potential with Passive Microwave Measurements." Water Resources Bulletin, American Water Resources Association, Vol. II, No. 5, pp.892-907.
3. Newton, R.W., "Microwave Remote Sensing and Its Application to Soil Moisture with Microwave Radiometers-II," Technical Report RSC 81, Remote Sensing Center, Texas A&M University, College Station, Texas, January 1977.
4. Ulbay, F.T., J. Cihlar and R.K. Moore, "Active Microwave Measurements of Soil Water Content," Remote Sensing of Environment, Vol. 3, 1974, pp. 185-203

The REMOTE SENSING CENTER was established by authority of the Board of Directors of the Texas A&M University System on February 27, 1968. The CENTER is a consortium of four colleges of the University; Agriculture, Engineering, Geosciences, and Science. This unique organization concentrates on the development and utilization of remote sensing techniques and technology for a broad range of applications to the betterment of mankind.